ISSN 1027-5495. Functional Materials, 28, No.4 (2021), p. 720-728.
doi:https://doi.org/10.15407/fm28.04.720

Corrosion resistance of reinforced concrete based on different cementitious materials

Tao Sun[1,2]

[1]School of Architectural Technology, Jiangsu Jianzhu Institute, Xuzhou, 221116 Jiangsu, China
[2]School of Mechanics and Civil Engineering, China University of Mining & Technology, Xuzhou, 221116 Jiangsu, China

Received July 23, 2021

Research on the corrosion of steel rods in concrete structures has been carried out. Four types of samples were studied: reinforced concrete; with epoxy resin coatings; and with conventional Portland cement and magnesium cement as binders. Corrosion resistance was studied by electrochemical method, resistance method, internal rapid corrosion test and field tests. The results show that the addition of mineral additives such as mineral powder, fly ash and silica fume to Portland cement can improve the complex performance of marine concrete, and the composite additive has a better effect on increasing the resistance of concrete to chloride ion corrosion than a single additive.

Keywords: cementitious materials, reinforced concrete, chloride ion diffusion coefficient, durability, corrosion resistance.

Корозійна стійкість залізобетону на основі різних цементних матеріалів. *Тао Сун*
Проведено дослідження корозії стальних стержней у бетонних конструкціях. Дослідження проводилися на чотирьох типах зразків: залізобетонні; з покриттями із епоксидної смоли; зразками із звичайного портландцементу та з магнієвого цементу в якості в'яжучих матеріалів. Корозійну стійкість вивчено електрохімічним методом, методом опору, внутрішнім експрес-тестом на коррозію та польовими випробуваннями. Результати показують, що додавання мінеральних добавок, таких як мінеральний порошок, летка зола та мікрокремнезем, до портландцементу, може покращити комплексні характеристики бетону. Композитна добавка краще впливає на підвищення стійкості бетону до хлоридно-іонної корозії, ніж проста добавка.

Проведены исследования коррозии стальных стержней в бетонных конструкциях. Исследования проводились на четырех типах образцов: железобетонные; с покрытиями из эпоксидной смолы; образцы из обычного портландцемента и из магниевого цемента в качестве вяжущих материалов. Коррозиционная стойкость изучалась электрохимическим методом, методом сопротивления, внутренним экспресс-тестом на коррозию и полевыми испытаниями. Результаты показывают, что добавление минеральных добавок, таких как минеральный порошок, летучая зола и микрокремнезем, к портландцементу может улучшить комплексные характеристики бетона. Композитная добавка лучше влияет на повышение устойчивости бетона к хлоридно-ионной коррозии, чем простая добавка.

1. Introduction

Durability of the reinforced concrete structure means the ability of the structure to maintain its safety, functionality and appearance [1]. This also means that the deterioration of the material properties of the structure within a predetermined time under the action of chemical, biological or other unfavorable factors will not lead to

unacceptable failure probability of the structure [2, 3]. When calculating the strength of reinforced concrete structures, the time point of corrosion of steel bars is usually taken as the end point of the calculation of durability. Reducing the diffusion rate of chloride ions in concrete or increasing the critical concentration of chloride ions causing corrosion of steel bars is of great significance to improve the durability of reinforced concrete structures [4, 5].

With the widespread use of concrete structures, the operating environment becomes more and more varied, and it is inevitably influenced by various external environments, leading to corrosion and damage. Cement concrete is an alkaline material with pH value usually higher than 12, which is easily eroded in the acidic medium, including acid rain, acidic groundwater or acidic soil, acidic industrial sewage and biological acid in sewage pipes, etc. [6, 7]. In [8], the characteristics of damage and destruction of ordinary concrete and high-strength concrete in 5 %, 10 % solution and brine of a salt lake were studied. The results show that: in the Na_2SO_4 solution, ions SO_4^{2-} lead to expansive failure of concrete, and in the $MgSO_4$ solution and salt lake brine, the combined action of corrosive ions SO sub 4 sup 2- and Mg^{2+} in solution will lead to cracking of the concrete. Data of [9] show that the influence of the content of impurity ions of sulfate and magnesium on the strength of concrete is greater than that of a water binder; sulfate and magnesium ions do not directly corrode the steel bar, but indirectly affect the destruction of the passivation film of the steel bar if chloride ions are involved. In [10], corrosion potential, linear polarization, electrochemical impedance spectroscopy and cyclic polarization were used to compare the corrosion behavior of rebar in C50 and C80 concrete. The research shows that chloride ions in C80 concrete mixed with silica fume reaches the surface of steel bar slowly, which indicates that the corrosion resistance is better. The authors of [11] used the method of computer simulation taking into consideration the concrete mix ratio, structural characteristic parameters, building construction environment and other conditions; the forecast of the resource of reinforced concrete structures based on carbonization and chloride-ionic corrosion of steel rods has been studied. The authors of [12] investigated the resistance of concrete reinforced with magnesium cement under conditions of one-factor erosion of mountainous soil. It was found that concrete reinforced with magnesium cement, after prolonged erosion by seawater salt, has excellent corrosion resistance, but reinforcement is corroded to some extent. In [13], the resistance method was used to study and analyze the influencing factors of steel bar corrosion, such as the relative humidity of the environment, the invasion of chloride ions in concrete, etc.; also the method of mathematical simulation was used, and the corrosion of steel bar was estimated according to the results of the resistance method, mathematical calculations and potentiodynamic method.

At present, magnesium cement concrete is mainly used as a non-load-bearing structural material of buildings, and its research mainly focuses on plain concrete specimens. In order to expand the application of magnesium cement concrete products in the field of building structures, two kinds of cementitious materials and two kinds of reinforced concrete specimens in the protection state of steel bars were made in this experiment, and their corrosion resistance was studied by prolonged immersion in a binder solution of chloride, magnesium salt and sulfate.

2. Experimental

2.1. Raw materials and mix design

The cement produced by China Cement Plant meets the requirements of various performance indexes of General Portland Cement. Slag micropowder is obtained from C95 grade mineral powder produced by a company in Shanghai, with density of 2.9 $g \cdot cm^{-3}$, specific surface area of 420 $m^2 \cdot kg^{-1}$ and total activity (24 d) of 101 %. Silica fume: the mass fraction of SiO_2 is 91 %, the specific surface area is 1.8×10^4 $m^2 \cdot kg^{-1}$, and the total activity (24d) is 121 %, was produced by Norwegian Ekeng Company. Sulphuric acid: 98 % by mass, density 1.84 $g \cdot cm^{-3}$, produced by Shanghai Sulphuric Acid Plant.

The research shows that replacing 20 %–30 % cement with mineral powder can improve the acid corrosion resistance of concrete [14]. The addition of silica fume can also improve the acid corrosion resistance of cement paste specimens [15]. According to this, four groups of composite cementitious materials systems were designed for research in this experiment: Mg–B, P.O–B, Mg–GHT and P.O–GHT, among which Mg–

Table. Part number and mix proportion design

Test piece number	Cement	Coarse aggregate	Fine aggregate	Grade I flyash	Water	Water reducing agent	Phosphoric acid	Magnesium chloride	Magnesium oxide	Rustinhibitor
Mg–B	–	22.1	12.4	1.33	2.93	0.37	0.08	2.88	7.76	–
P.O–B	7	17.5	17.5	2.26	2.26	1.28	–	–	–	0.81
Mg–GHT	–	22.1	12.4	1.33	2.93	0.37	0.08	2.88	7.76	–
P.O–GHT	7	17.5	17.5	2.2	6	2.6	6	1.28	–	–

B, P.O-B, Mg-GHT and P.O-GHT, respectively, are samples of magnesium-reinforced cement and conventional uncoated and epoxy-coated Portland cement. The specimen number and mix proportions are shown in Table.

2.2. Main experimental methods

2.2.1. X–ray diffraction

First, the sample was placed in a vacuum drying oven, dried in vacuum at 50°C for 24 h, then it was ground in an agate mortar, and the ground sample was passed through a sieve with round holes of 45 μm.

X-ray diffraction analysis was carried out using a fully automatic X-ray diffractometer d/max-iii from Nippon Science. The measurement conditions are: Cu target (some samples are Co target), graphite monochromator, voltage 40 kV, current 30 mA, and scanning speed 5 degrees/minute.

2.2.2. Determination of specific surface area of cementitious materials

The specific surface area of cement, fly ash and slag powder are determined in accordance with the provisions of Methods for Chemical Analysis of Cement. The specific surface area of silica fume is measured by nitrogen adsorption method, and the equipment used is an SSA-3500 specific surface area tester.

2.2.3. Determination of chemically bound water of cementitious materials

Sample preparation: the raw materials are mixed according to a certain proportion, and after stirring, the samples for hydration tests were made in the form of small pieces of pure cellulose measuring 2 cm×2 cm×2 cm; after curing to the specified age in accordance with the test conditions, the surface layer was removed and the middle part of the sample was taken. Immediately after sampling, the sample was impregnated with absolute ethanol to stop hydration, while the absolute ethanol was changed twice regularly. After extraction, the hydrated sample was wet milled with absolute ethyl alcohol and the hydrated sample suspension was filtered under vacuum. Then the slurry was put into a vacuum drying oven and dried at 50°C for 24 h. The dried sample was tested for chemically bound water.

Determination of bound water: three samples are weighed, which have been hydrated and dried in vacuum at each age, each of which is about 1 g (±0.0005 g), and dried at 105°C for 6 h. The dried sample is heated to 950°C in a high-temperature electric furnace at a rate of 15°C/min, and kept at a constant temperature of 950°C for 1 h. Then, the sample is placed in a dryer to be cooled to room temperature and weighed, and the combined water of the sample is taken as the average of the three samples.

2.2.4. Evaluation index of concrete durability

Generally, the durability test method of concrete is used, but the damage test method is destructive to the specimen and unrepeatable to the same specimen, which makes it impossible to carry out a long-term test for the same specimen. Because of the heterogeneity of concrete itself and the irreproducibility of different specimens, this will lead to inevitable experimental errors, and the damage test requires a lot of manpower and material resources. Therefore, the durability of concrete is studied by means of nondestructive testing.

According to the relative dynamic elastic modulus specified in Test Methods for Long-term Performance and Durability of Ordinary Concrete [16], its calculation formula is as follows (1):

$$E_r = \frac{E_t}{E_0} = \frac{V_t^2}{V_0^2}, \quad (1)$$

in which: E_{er} is the relative dynamic elastic modulus of materials; E_0, V_0 are, respectively, initial dynamic elastic modulus and ultrasonic velocity of materials before testing; E_t, V_t are respectively, dynamic elastic

modulus and ultrasonic velocity of materials after a certain age.

An electronic scale with a sensitivity of 0.1 g was used to test the quality of the workpiece. The calculation formula is as follows:

$$W_r = \frac{W_n}{W_0} \times 100\% \quad (2)$$

in which: W_r is the relative mass (%) of the test piece measured at the N time; W_n the mass of the test piece measured at the time (kg); W_0 is the mass of the test piece measured initially (kg).

In this test, the indices of concrete durability obtained in [17], ω_1, ω_2 were chosen as the evaluation parameters of concrete durability. The calculation formula of relative dynamic elastic modulus evaluation parameter ω_1 is as follows:

$$\omega_1 = \frac{E_t = 0.6}{0.4}. \quad (3)$$

When $\omega_1 < 0$, the relative dynamic elastic modulus is lower than 60 %, and the failure is reached. When $0 < \omega_1 < 1$, the relative dynamic elastic modulus is lower than the reference value, and the failure is not reached. When $\omega_1 > 0$, the relative dynamic elastic modulus increases compared with the reference value.

The calculation formula of the relative quality evaluation parameter ω_2 is as follows:

$$\omega_2 = \frac{M_r{=}0.95}{0.05} \quad (4)$$

When $\omega_2 < 0$, the relative mass is less than 95 %, and the damage is achieved. When $0 < \omega_2 < 1$, the relative mass is lower than the reference value, and the damage is not reached. When $\omega_2 > 1$, the relative mass increases compared with the reference value.

Electrochemical impedance spectroscopy is an important research method to study the electrode reaction kinetics and reveal the corrosion and corrosion inhibition mechanism of materials [18]. To study the corrosion of reinforced concrete, sinusoidal AC signals with small amplitude in a certain frequency range are applied to a reinforced concrete system; the periodic characteristic of the ratio of the AC potential to the current signal is measured, as well as a complex flat impedance diagram, impedance mode-frequency diagram and phase angle-frequency diagram are measured [19, 20].

In this paper, the impedance spectrum obtained in the electrochemical experiment is processed by calculating the equivalent circuit using the Zman software, and a numerical solution of each parameter of each coupled element is obtained to finally obtain the polarization resistance R_p, solution impedance R_s and capacitance C of the steel bars.

$$R_p = \frac{2|Z(\omega)|}{\tan(\theta)}. \quad (5)$$

$$C = \frac{1}{\omega R_p}. \quad (6)$$

In this electrochemical test, the material density is 7.8 g/cm^3, the electrode area is 18 cm^2, the scanning rate is 0.167 mv/s, the electrochemical equivalent of steel bar is 28 g, and the test environment temperature is about 25°C. In order to avoid interference during the test, the specimen is placed in a shielding box connected with the earth.

2.2.5. Immersion corrosion test

In this article, the authors selected a sulfuric acid solution for the study and applied the full immersion method, in which each group of samples is immersed in a reservoir of water, and each sample of a clean suspension is immersed in 2 liters of solution. The initial H^+ concentration of the acid solution is 0.01 mol·L^{-1}, pH and the pH value is 2. The level of the impregnating solution is more than 2 cm above the upper surface of the sample, and the distance between each sample is at least 5 cm. The distance between the bottom surface of the sample and the bottom of the sink should be at least 2 cm to ensure that each sample is completely saturated. The reaction between the hydration products of alkaline cement and acid consumes H^+, so the residual H^+ concentration of the solution is measured by titration every 24 h.

Then, the acid solution was supplemented with concentrated sulfuric acid until H^+ reached the initial concentration of 0.01 mol·L^{-1} . During the test, the pH value of the corrosion solution could be controlled in the range of 1.9 ~ 2.4. The solution was changed every 7 days, and the acid consumption, mass loss and corrosion depth at specific corrosion age were measured.

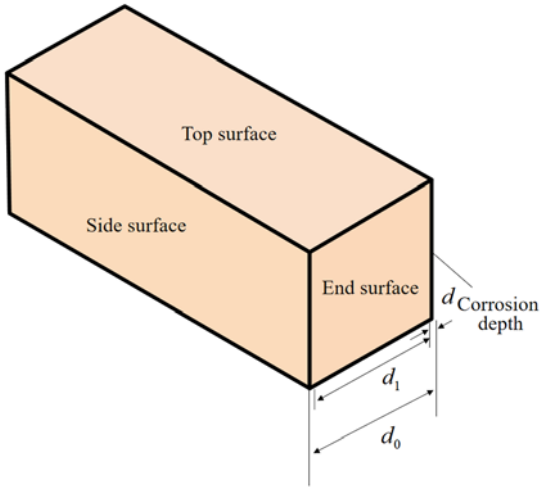

Fig. 1. Schematic diagram of acid corrosion depth of clean slurry specimen.

2.2.6. Measurement and calculation of corrosion depth

Nowadays, scientists at home and abroad often use loss of strength to characterize the acid resistance of mortar and concrete. However, the measurement of strength is discrete, especially when the degree of corrosion is low, so it is difficult to express the acid resistance of the samples only by the change in strength, and it is not suitable for analyzing the kinetics of corrosion [21]. Therefore, in this paper, we take the corrosion depth as the main index, evaluate the acid resistance of hardened cement paste with composite cementitious materials, and analyze its corrosion kinetics.

In this study, a steel brush (or sandpaper or file) was used to scrape off the loose corrosion layer on the side of the specimen, and the thickness of the specimen after scraping off the corrosion layer was measured by a vernier caliper (with an accuracy of 0.02 mm), and compared with the initial thickness of the specimen; and the corrosion depth d (mm) was determined by calculation, as shown in Fig. 1. In the figure, d_0 is the initial thickness, mm; d_1 is the thickness after corrosion, mm.

The corrosion depth is calculated according to formula (1), and is accurate to 0.01 mm:

$$d = \frac{d_0 - d}{2}. \quad (7)$$

Dashed lines are marked before measurement to ensure consistency of measurement points before and after measurement. 5 points are measured at equal intervals for each specimen. After removing the maximum and minimum values, the average value is taken as the corrosion depth value of the specimen, and the average value of the corrosion depth of the three specimens is taken as the representative value of the corrosion depth of this group of specimens.

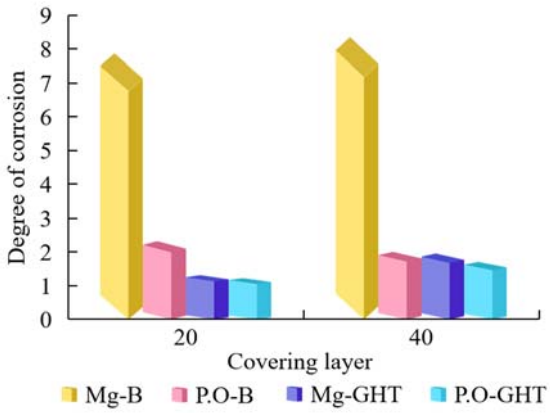

Fig. 2. Corrosion degree of reinforced concrete with different protective layers in 350d.

3. Results and discussion

3.1. Study on corrosion law of exposed steel bars with different protective layers in concrete

The self-corrosion potential, corrosion rate and corrosion current density of bare reinforced concrete with four ratios of 20 mm and 40 mm protective layers in the coupling environment of chloride, sulfate and magnesium salt were analyzed.

Depending on the corrosion condition of exposed steel bars, the best cover thickness of the steel bars in each concrete is estimated. With the corrosion current density of reinforcement as the evaluation index, the corrosion degree of reinforcement after long-term immersion for 350d is shown in Fig. 2.

It can be seen from Fig. 2 that the corrosion degree of the exposed steel bars varies with the thickness of the protective layer. Therefore, for magnesium cement concrete and portland cement concrete with ratio 1, the exposed steel bars have high corrosion when the protective layer is 20 mm and 40 mm; while the exposed steel bars in portland cement concrete with ratio 2 have medium corrosion, when the protective layer is 20 mm and high corrosion, when the protective layer is 40 mm. Through the above analysis, it can be concluded that the bare steel bar has no ability to resist bittern corrosion in magnesium cement concrete.

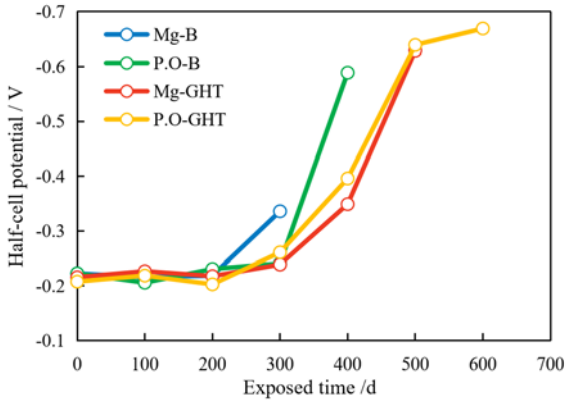

Fig. 3. Influence of exposure time on corrosion potential of slag reinforcement.

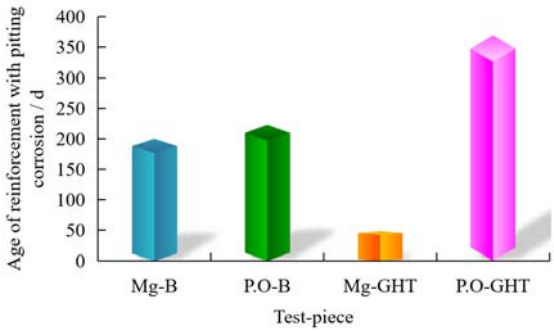

Fig. 4. Influence of cementitious material composition on durability of reinforced concrete structures.

3.2. Influence of fly ash content on corrosion potential of steel bars

Changes in the corrosion potential of steel rods in fly ash concrete specimens at different test times are shown in Fig. 3. It can be seen from Fig. 3 that the corrosion potential of steel bars increases gradually with the extension of exposure time, then decreases gradually, and finally decreases rapidly. Since polycarboxylate superplasticizer has a certain inducing effect, a certain number of bubbles will remain at the interface between steel bars and concrete during the concrete forming process, and the steel bars in concrete do not form a stable passivation film in a short time, so the corrosion potential is about −250 mV. With the prolongation of the exposure time and the enhancement of the stability of passivation film, the corrosion potential of steel bars began to move positively, which was about −200 mV.

When the exposure time of concrete specimens with 30 % fly ash reaches 400 days, the passivation film of steel bars in the specimens will be destroyed and the corrosion potential of steel bars will decrease rapidly; while the corrosion potential of concrete specimens without fly ash will decrease rapidly when the exposure time is 200 days. Therefore, the reasonable use of fly ash to replace part of cement can prolong the damage time of the steel bar passivation film in concrete and improve the durability of the reinforced concrete structure. However, within the scope of this test, the best content of fly ash is 30 %, and the excessive content of fly ash will reduce the durability of reinforced concrete specimens.

3.3. Influence of cementitious material composition on durability of reinforced concrete

Generally, the pitting time of steel bars in concrete is regarded as the end point of durability life of the reinforced concrete structure, and the influence of the cementitious material composition on durability of reinforced concrete is shown in Fig. 4.

It can be seen from Fig. 4 that after replacing part of cement with fly ash or slag, the pitting time of reinforcement can be prolonged, thus improving the durability of reinforced concrete. At the same time, it can be seen from the figure that the pitting time of steel bars in concrete increases first and then decreases with an increase in the fly ash and slag content.

Replacing part of the cement with an additive reduces the critical concentration of chloride ions during steel corrosion, but also reduces the diffusion coefficient of chloride ions in concrete, improves concrete resistivity and reduces the corrosion rate of steel bars. Therefore, replacing part of cement with an additive has a positive effect on the durability of reinforced concrete.

3.4. Effect of compound admixture on chloride ion diffusion coefficient

Corrosion and expansion of steel bars in concrete caused by chloride in marine environment is one of the most important reasons for the damage of concrete structures. Therefore, reducing the diffusion rate of chloride ions in concrete and prolonging the time required for chloride ions to reach steel bars are one of the important means to improve the service life of marine structures. The chloride ion diffusion coefficient is an important parameter reflecting the resistance of concrete structures to chloride ion permeability; so, the problem of effec-

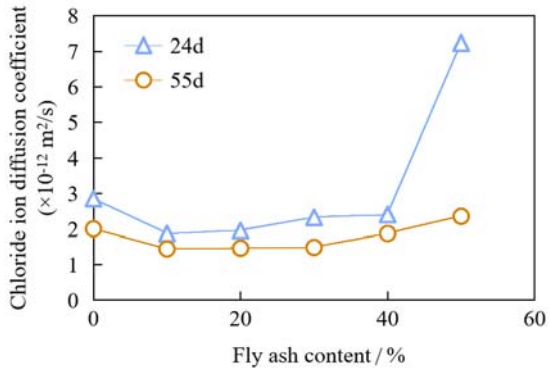

Fig. 5. Influence of fly ash content in composite admixture on chloride ion diffusion coefficient of concrete.

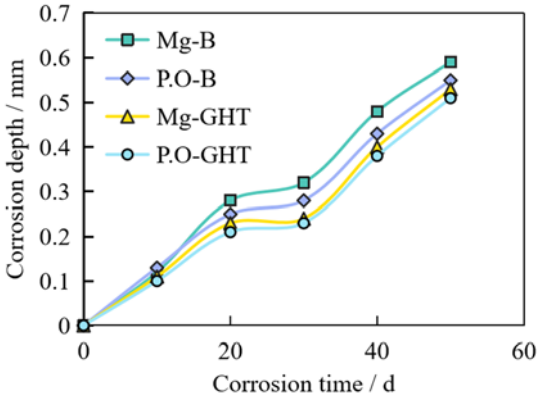

Fig. 6. Immersion corrosion depth of clean slurry specimen.

tive reducing the chloride ion diffusion coefficient in concrete is one of the focuses and hotspots in the durability research of marine concrete structures at present.

To study the compressive strength and the chloride ion diffusion coefficient of concrete specimens, the specimens with 50 % of the total amount were selected. Fig. 5 shows the influence of fly ash content in the composite admixture on the chloride ion diffusion coefficient of concrete.

It can be seen from Fig. 5 that with the total amount of composite admixture of 50 %, the chloride ion diffusion coefficient of concrete specimens in different curing ages first decreases and then increases with an increase in the fly ash content in the admixture, but they are all higher than in samples with a 50 % fly ash content.

The concrete specimens with the lowest chloride ion diffusion coefficient at different curing ages are also different, and the specimens with the 10 % fly ash content at 24 days age have the lowest chloride ion diffusion coefficient. The main reason is that the hydration activity of fly ash is different from that of slag. Since the activity of fly ash is lower than that of slag, prolonging curing age is most beneficial to improve the hydration of fly ash in composite admixture.

3.5. Corrosion kinetics analysis

When testing for acid corrosion of hardened cement paste with composite cementitious materials, the corrosion depth and corrosion time are fitted, and the fitting curve is shown in Fig. 6.

It can be seen that there is a good correlation between the fitted curve equation and the test results, based on which, the relationship between acid corrosion depth d and corrosion time t under the test conditions is summarized:

$$d = Kt^n. \tag{7}$$

Where K, n is the test fitting index, which depends on the composition of cementitious materials and test conditions; t is corrosion time.

The equation of corrosion velocity v_d with corrosion depth as the index can be obtained by differentiating the time t from equation (8):

$$v_d = Knt^{n-1}. \tag{8}$$

According to the experimental index n, which is about 0.8, it can be seen that the corrosion rate v_d is a decreasing function of the corrosion time t, which is consistent with the phenomenon that the acid consumption rate decreases.

It can be seen from the mathematical expression of v_d that the corrosion rate decreases with the corrosion time. The investigation of a concrete platform corroded by an acidic river in [22] also shows that the initial corrosion rate of concrete is faster, and the later corrosion gradually slows down. This may be due to two factors. First, the degree of cement hydration increases with age, the suspension gradually becomes dense and stable, and its corrosion resistance increases accordingly. Second, the protective effect of the outer anticorrosive layer slows down the penetration of the corrosive medium to a certain extent. Acidic medium destroys the cement gel through dissolution, which deteriorates the properties of cement-based materials. The corroded layer formed as a result of dissolution is loose, peels off easily and loses its cementability and bearing capacity. How-

ever, the corroded layer can avoid the direct contact between internal cement stone and acid, and has the function of slowing down corrosion. The relationship between corrosion depth and corrosion time of four kinds of composite cementitious materials in sulfuric acid solution with pH = 2 is that the corrosion rate decreases with an increase in the corrosion time.

4. Conclusions

Chloride ion corrosion of reinforced concrete in marine environment includes two key parameters: chloride ion diffusion coefficient in concrete and chloride ion critical concentration which causes corrosion of reinforced concrete. In this study, the effects of the above factors on chloride ion corrosion of reinforced concrete were studied under different environmental conditions, using different cements and fly ash and slag as mineral admixtures.

The electrochemical corrosion behavior of epoxy-coated steel bars with different protective layers in magnesium cement concrete and Portland cement concrete was preliminarily studied using polarization curves and AC impedance spectroscopy under corrosion environments of chloride, sulfate and magnesium salt. It was concluded that the epoxy-coated steel bars in magnesium cement concrete and Portland cement concrete had low corrosion when the protective layers were 20 mm and 40 mm.

The fly ash and slag were mixed to replace part of cement. At the age of 24 days, when the total amount of mixed cement is 50 %, the chloride ion diffusion coefficient of concrete specimen decreases at first and then increases with increasing fly ash content in the admixture. The chloride ion diffusion coefficient is the lowest for the specimen with 10 % fly ash. The influence of admixture on the chloride ion diffusion coefficient is mainly due to the fact that the composite cementitious material system effectively reduces the porosity and average pore diameter of concrete, thus reducing the chloride ion diffusion coefficient.

The durability of reinforced concrete increases first and then decreases with an increase in the fly ash and slag content in cementitious materials. The resistivity of concrete and the charge transfer resistance of steel bars increase first and then decrease, while the corrosion rate of steel bars decreases first and then increases with an increase in the fly ash or slag content.

The relationship between acid corrosion depth and corrosion time of the hardened cement paste of cementitious materials is that the corrosion rate decreases with increasing corrosion time.

The study of the strength of reinforced concrete is a complex and lengthy process, because the mechanism of its corrosion is more complicated, especially in the environment of the combined action of various aggressive salt solutions. Therefore, it is of great significance to study magnesium cement reinforced concrete. However, magnesium cement concrete itself causes some corrosion of steel bars, so if we want to popularize the use of magnesium cement concrete, we must first solve the steel bar corrosion problem. However, studies of the corrosion behavior of reinforced concrete with different proportions under the combined action of chlorides, sulfates and magnesium salts are still insufficient, and they serve only as a guideline for future work in this area.

Acknowledgements. This work is from "333 Project" Supported by Scientific Research of Jiangsu Province in 2018 (No. BRA2018343).

References

1. Yongmin, Yang, Tongsheng et al., *J. Therm. Anal. Calorimetry*, **139**, 1903 (2020).
2. L.Hou, B.Zhou, S.Guo et al., *Constr. Build. Mater.*, **198**, 278 (2019).
3. Chuhongqiang, PAN, Congling et al., *J. Wuhan Univer. Technol.–Mater. Sci.)*, **34**, 129 (2019).
4. H.Chu, C.Pan, C.Xiong et al., *J. Wuhan Univer. Technol.–Mater. Sci. Ed.*, **34**, 1127 (2019).
5. A.Afshar, S.Jahandari, H.Rasekh et al., *Constr. Build. Mater.*, **262**, 120034 (2020).
6. A.M.Atta, N.Ali, M.H.Taman, *Composites, Part B Engin.*, **166**, 341 (2019).
7. M.Daniyal, S.Akhtar, A.Azam et al., *Arabian J. Sci. Engin.*, **45**, 4369 (2020).
8. Y.Yan, H.Liang, Y.Lu et al., *Constr. Build. Mater.*, **269**, 121283 (2020).
9. F.Almeida, A.Sales, J.P.Moretti et al., *Constr. Build. Mater.*, **226**, 72 (2019).
10. H.Fakhri, K.A.Ragalwar, R.Ranade, *Constr. Build. Mater.*, **224**, 850 (2019).
11. W.Zheng, M.Zou, Y.Wang, *J. Build. Struct.*, **40**, 28 (2019).
12. P.Ghoddousi, M.Haghtalab, A.Javid, *Cement Concrete Compos.*, **121**, 104077 (2021).
13. R.Dineshkumar, P.Balamurugan, *Innovative Infrastruct. Solut.*, **6**, 1 (2021).
14. V.Kumar, D.R.Prasad, *Adv. Concrete Constr.*, **7**, 75 (2019).
15. Y.Xu, H.Zhang, Y.Gan et al., *Additive Manufacturing*, **39**, 101887 (2021).

16. S.Permeh, K.Lau, M.Duncan et al., *Mater. Struct.*, **54**, 143 (2021).
17. H.Lin, Y.Li, Y.Li, *Constr. Build. Mater.*, **197**, 228 (2019).
18. X.Hao, X.Zhao, B.Huang et al., *J. Mater. Engin. Performance*, **29**, 4446 (2020).
19. B.Xya, W.Xuan, C.Yang et al., *J. Mater. Res. Technol.*, **9**. 12378 (2020).
20. Fengjiao Jiang, Gongzhi Yu, Ce Liang et al., *Functional Materials*, **28**, 114 (2021).
21. M.Gawda, P.Jelen, M.Bik et al., *Appl. Surf. Sci.*, **543**, 148871 (2020).
22. H.Tamai, Y.Sonoda, J.E.Bolander, *Constr. Build. Mater.*, **263**, 120638 (2020).
23. Q.S.Banyhussan, G.Yildirim, Q.Anil et al., *Struct. Concrete*, **20**, 1036 (2019).
24. F.Jiang, G.Jiang, W.Song et al., *Functional Materials*, **27**, 730 (2020).